IOSR Journal of Applied Physics (IOSR-JAP)
e-ISSN: 2278-4861.Volume 10, Issue 2 Ver. III (Mar. – Apr. 2018), PP 65-77
www.iosrjournals.org

A Cross-Bar,Bi-Periodicstructure for Compact Electron Accelerators

A. V. Smirnov[1], E. A. Savin[2]
[1]*RadiaBeam Systems LLC, 1713 Stewart St., Santa Monica, CA 90404, US*
[2]*National Research Nuclear University "MEPhI", Moscow, 115409, Russian Federation*
Corresponding Author:A. V. Smirnov1

Abstract : *A tubular cross-bar and cross-rod (alsocalled "jungle-gym") type of accelerating structure isrevisitedherefor compactelectronlinacsandMicroLinacs. It consists of ametal tube loadedperiodically by rods (or bars withbeam aperture) crossed at 90 degrees angle. The structure enables a wide range of phase velocities (including non-relativistic), a widebandwidthallowing large number of cells(for standing wave mode) or short filling time (for traveling wave mode) due to performance similaritywithbi-periodic structures.Single-section structure having up to hundredcellsisanalyzed.Beamdynamicsand vacuum aspects of the structure and MicroLinacperformanceare considered. Capture enhancementwith the rods made frommildsteelwhenusingexternalsolenoidfocusingisdemonstrated as well.*

Keywords: *accelerator, electrons, RFlinac, synchronism, wave.*

Date of Submission: 23-04-2018 Date of acceptance: 10-05-2018

I. Introduction

Linear accelerators of electrons (linacs) are employed in a wide variety of applications, including radiography and sterilization, radiolysis and imaging, modification of materials and testing of semiconductor electronic components for space applications. Among emerging applications is driving table-top sub-mm wave sources [1] and replacement of radionuclide sources [2] to improve public security and prevent the diversion of radioactive material for radiation dispersion devices. A challenging specific of such a replacement is inexpensive, portable, easy-to-manufacture linac system delivering electrons with energies from a fraction of 1 MeV to severalMeVs. The bremsstrahlung X-rays produced by the electron beam on a high-Z converter at the end of the linac may match the penetration and dose rate of a radionuclide source to be substituted.

As a rule classical linac system is rather expensive and not portable.MicroLinac technology originally proposed at SLAC [3]employsa compact X-band linear accelerator powered by an inexpensive,low power, magnetron [4,5]. However, to make the MicroLinac concept suitable for a wider scope ofapplications, the compact linac technology needs to be advanced to reduce further cost, weight, and dimensions.A compact modification may employ of a light-weightmodulator, using, e.g., a transformer-free Marx scheme with array of isolated gate bipolar transistors (IGBTs). Such a modulatormakes development of a light-weight linac and focusing structures even more important.

First practicalstep towards compact X-band MicroLinacs has been made by utilizing high-impedance, all-copper, multi-cell structures [4,6]. A bi-periodic part of a MicroLinac structure employs side [6] or on-axis [4] coupling cells enabling a somewhat substantial bandwidth and number of cells to achieve about 1 MeV beam energieswithin a single section at limited power supply (sub-MW in X-band). However, fabrication of a multi-cell, tapered MicroLinac structure remains rather expensive and time consuming. It includeshigh precision machining,cold-testing and re-machining of the cells, testing of the clamped assembly, multi-step brazing, andindividual cell tuningof the brazed assembly.

One unexplored opportunity for eased fabrication of a MicroLinac is using of a tubular cross-bar or cross-rod type of linac structure. Early studies on the structure were carried out at the Hansen laboratories at Stanford. Probably first time such "jungle-gym" and "easitron" structureswere mentioned as a candidate for accelerator applications among the backward-wave variants of the Stanford two-mile accelerator project [7]. A four-cell,cross-rod, UHF-bandstructure was used for a long period in the Cornell electron synchrotron [8].More detailed study of the cross-rod type periodic structure was performed in Los Alamos National Laboratory (LANL, [9]). Next interesting implication of this structure is related toits anomalous dispersion enabling so-called "inversed wakefields" forerunning the charge when group velocity exceeds charge velocity [10].

Attractive advantages of this structure are its relatively simple, mechanically rigid construction, large-error tolerances, ease of cooling, compactness, and reasonable shunt impedance.

In the next section we revisit performance of elementary cells of cross-bar and cross-rod structures. In Section 3 we present and analyze RF performance of two multi-cell, single-section, X-band structures for replacement of Ir192 and Cs137 radioisotope. Also we model vacuum quality along the structure. Section 4 includes beam dynamics simulationsincludingfocusing option enhanced with mild steel pins (rods).

The electromagnetic and beam dynamics simulationspresented below have been performed with the CST Studio Suite™[11] and ASTRA [12] codes. In all designs presented here we use ~9.4 GHz as the operation frequency, ~∅0.75" internal diameter of copper tubing for the tubular structure housing, and 3 mm beam aperture (square for cross rods and circular for cross-bar).

II. Cross-Bar And Cross-Rod Structure Cells

2.1. A structure with crossed pairs of cylindrical rods

Electromagnetic model of cross-rod structure cells designed for relativistic energies using circular pins (rods) is shown in Fig.1.One can see that this structure is composed from two superimposed periodic structures rotated by 90° with respect to each other. In general a bi-periodic structure becomes compensated when the stopband between two TM01 (or TM02 [13]) adjacent passbands disappears and the two modes acquire the same frequency for the given phase velocity. Important to note that unlike conventional compensated structures the structure geometry allows compensation for the two TM01 degenerate modes shown in Fig.1b,cautomatically at the π phase advance per geometric period due to different polarizations (degeneracy).

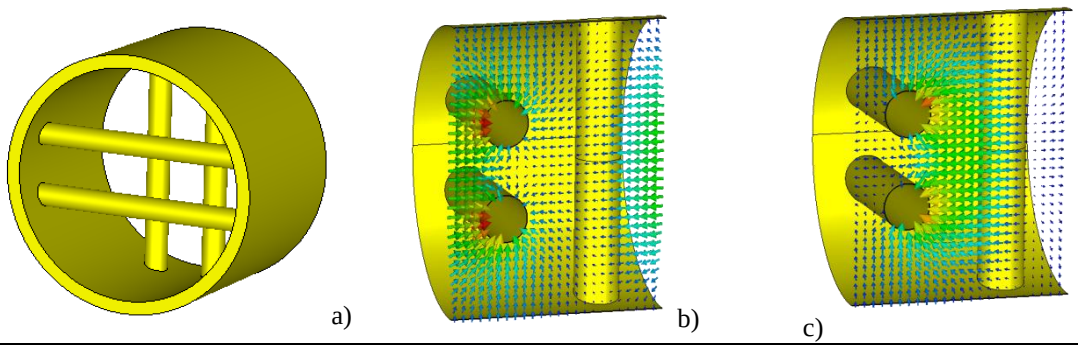

Fig.1: Cross-rod structure cell at 0.9c phase velocity (a).Two degenerate modes (b) and (c) at π phase advance and at the same frequency(enabling compensation effect).Cell length is $\beta_{ph}\cdot\lambda\cdot\theta/2\pi$, where θ is phase advance per cell.

Brillouin diagram and shunt impedance are simulated in Fig. 2 and Fig. 3 using a single cell model shown in Fig. 1 with periodic boundary conditions applied. The single cell simulation resultsareusedbelow to design a tapered structure composed from cells having different phase velocity.This is enabled by similarity between along periodic and a finite length structures in terms of inter-cell boundary conditions. Shunt impedance simulated as a function of phase velocity is given in Fig.3. One can see from Fig.2 that the simple design provides compensation by means of coupling between the two degenerate modes at 180° phase advance. Similar to the Andreev's disk-and-washer (DaW, [13]) and disk-and-ring (DaR, [14,15]) structures the interaction between the two overlapped passbands results to effective 90° phase advance in terms interaction with electron beam. Note at the crossing point (i.e. exactly at 180° phase advance) the effective shunt impedance that provides actual interaction with the charged particles is about twice that for each of the degenerate modes. That explains why the maximum shunt impedance of Fig.3 is nearly twice less than that in Fig.2b. In other words, the beam does not see the mode switching in the crossing point (see Fig.2b in the vicinity of that point).

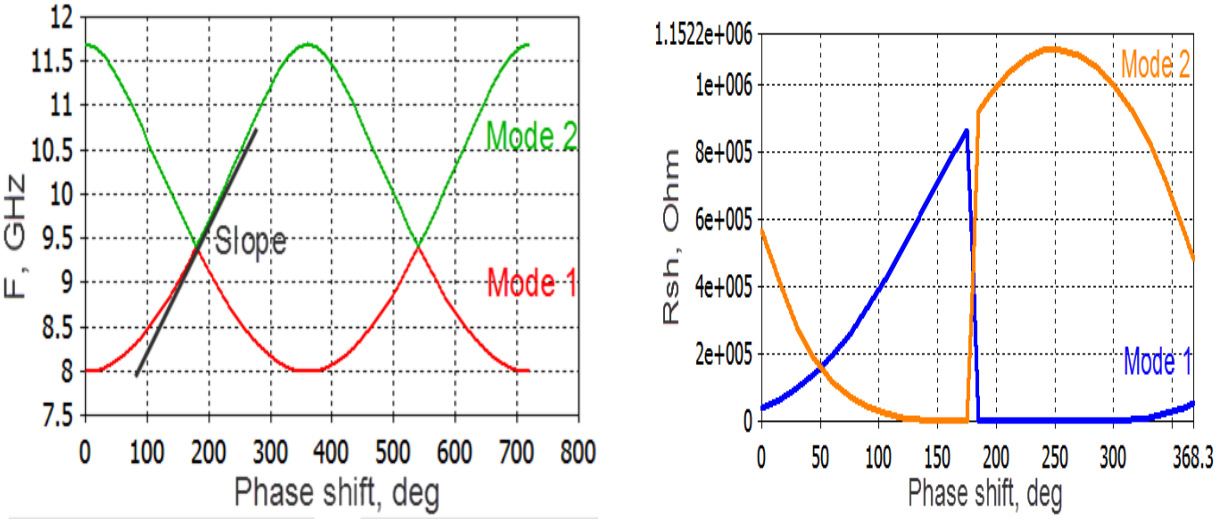

a) b)

Fig.2: Dispersion diagram (a) and shunt impedance (b) plotted vs. phase velocity simulated for two modes with compensation at θ=180° phase advance per geometric period for phase velocity ~0.9c. Calculated coupling coefficient is 36.3%.

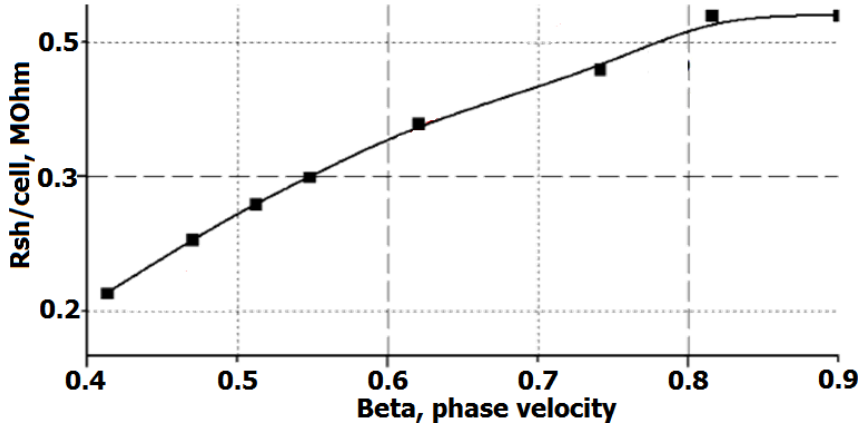

Fig.3: Shunt impedance per π-mode cell of cross-rod type (see Fig.1) simulated as a function of normalized phase velocity for only one of the degenerated modes at 180° phase advance per geometric period.

2.2. A structure with crossed non-cylindrical bars

Another variation of the design under scope is cross-bar structure shown in Fig.4. The structure dispersion and interaction efficiency are characterized in Fig.5.

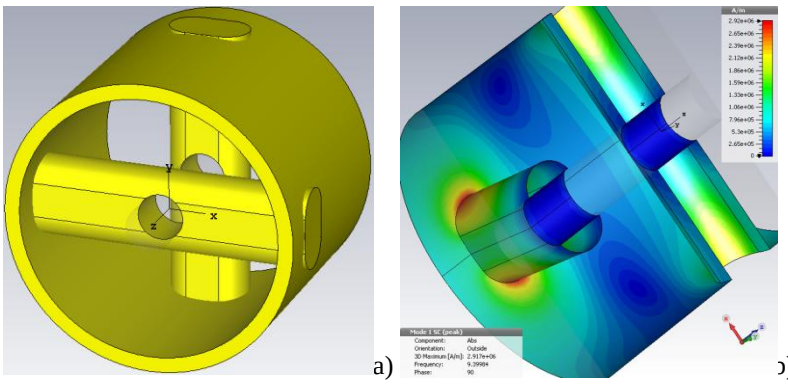

a) ɔ)

Fig.4: One period of cross-bar structure (a) and its surface currents (b) at 180° phase advance per geometric period and 0.945c phase velocity**.**

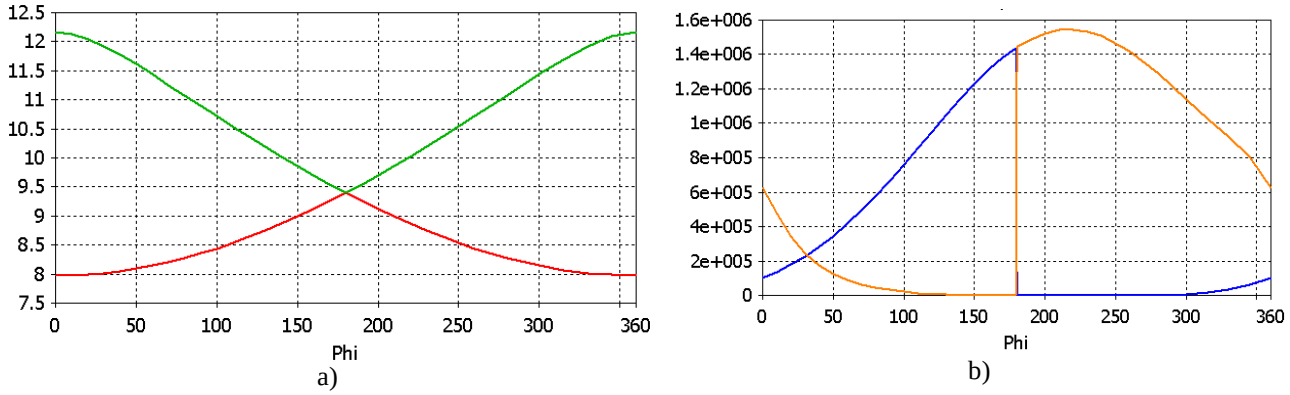

Fig.5: Characterization of a compensated cross-bar single cell of Fig.4. Brillouin diagram (GHz vs. degrees) for two TM01 modes (a); Shunt impedance (Ohms) plotted vs. phase advance (degrees) for the two modes (b). Calculated coupling coefficient is 39.5%.

Strong magnetic inter-cell coupling in the structure provides compensation the same wayas cross-rod structure (see Fig.2) with about the same group velocity. Thus the "jungle-gym" cross-rod (or cross-pin) and cross bar structures are very close to each other in terms of dispersion, bandwidth, group velocity, transverse dimension, vacuum conductivity, and possible coupler configurations. However, as it can be seen from Fig.5b the cross-bar structure enables noticeably higher shunt impedance (93 MΩ/m vs. 60 MΩ/m) at slightly higher group velocity (0.26c vs. 0.24c) for ~0.94c phase velocity. Another substantial difference is related to so-called overvoltage(discussed in Section 2.3).

From comparison of dispersion (a) and shunt impedance (b) plots of Fig.2 and Fig.5 for the two coupled modes one can find that the group velocity is positive unlike DaR structures [14,15]. That means that the coupling is dominated by electrical energy.

Note the cross-bar structure given in Fig.4 can be considered as a simplified version of a spoke cavity introduced in Argonne National Laboratory in the late 80s for superconducting proton and ion accelerators [16]. The spoke structures are designed to operate from 0.1c to 1c phase velocities [17,18] typically in UHF band. One importantfeature of a spoke structure is lower ratio of peak surface magnetic field to accelerating field: 4.2-7.5 mT/(MV/m) for β_{ph}=1-0.9 [17,19] vs. ~17 mT/(MV/m) for the cross-bars (at β_{ph}=0.945).

Note spoke cavities are optimized for operation at more than order lower frequencies. Therefore the geometric parameter defined as shunt impedance over Q-factor (R/Q) is also higher for spoke cavities (by factor of ~2.5). Scaling of a typical spoke structure to centimeter wavelengths of our interest would make the production cost of the structure with dozens of cells prohibitively high (if feasible at all) for large series of microlinacs, whereas beam aperture would be too small to be practical. Therefore the cross bar/rod structures considered here are perfectly suitable for long multi-cell and/or travelling wave structures unlike spoke cavities.

2.3. Overvoltage for cross-bar and cross-rod structures

The cross-rod or cross-bar structure can be considered for applications with substantial accelerating gradients especially for centimeter wavelengths. The capability of high gradient acceleration is defined by overvoltage defined as the ratio of the maximum surface electric field to the accelerating gradient (Emax/Eacc). The cross-rod structure of Fig.1 is optimized for maximum shunt impedance. The overvoltage for that structure is substantial and equals to 6.2 (for β_{ph}=0.9, and rod diameter 1.75 mm at f=9.4 GHz). The overvoltage can be decreased down to 4.55 for larger ∅3 mm rods at that frequency by sacrificing shunt impedance by ~15%. More efficient way to decrease the overvoltage is increase of accelerating gradient by means of using non-circular rods as shown in Fig.6. However, such a dramatic modification in general destroys the compensation effect leading to dramatic reduction of group velocity (down to zero). We found a configuration shown in Fig.6b that provides relatively moderate overvoltage 4.65 while keeping the compensation. The rod shape in Fig.6b was optimized to maximally decrease the overvoltage value while keeping shunt impedance close to that for the structure with circular rods with 1.75 mm diameter (see Fig.1).

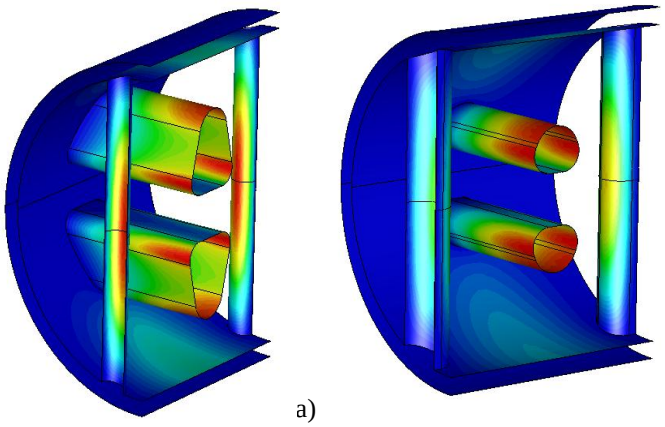

a) b)

Fig.6: Surface electric field distributions at optimized rods geometry for minimum overvoltage without compensation (a) and with compensation (b) producing Emax/Eacc values 3.5 and 4.65 respectively**.**

And finally we calculated the overvoltage for the cross-bar structure of Fig.4, which is Emax/Eacc=3 for β_{ph}=0.945 without special geometry optimization to further minimize Emax/Eacc. This value can be compared toEmax/Eacc≈3.7-2.67 for spoke cavity at β_{ph}=1-0.9 given in [17,19].Thus for higher gradient applications the cross-rod structure of Fig.1 is least suitable among structures considered here.

III. RF design of a long, multi-cell,single SW section

In this section we consider design and RF performance of the cross-rod type structure (see Fig.1) capable to accelerate electrons injected at ~14 keV energy up to ~1 MeV and 3.5-4 MeV energies using moderate RF power sources, namely less than ~130 kW and ~600 kW respectively. The cross-rod structure is chosen here solely due to simplicity of fabrication enabling usage of standard cylindrical pins. With properly designed high-Z target employed as bremsstrahlung converter the 1 MeV and 3.5-4 MeV electron energies allow to mimic X-rays produced by Ir192 and Cs137 radioactive sources respectively.

3.1. A 37-cell MicroLinac section

The CST RF model for ~1 MeV MicroLinac is shown in Fig.7. The design employs elliptical shape of the RF coupler allowing wider range of coupling coefficients. S11 curve and the operating mode profile along the section given in model of Fig.7are shown in Fig.8 and Fig.9 respectively.

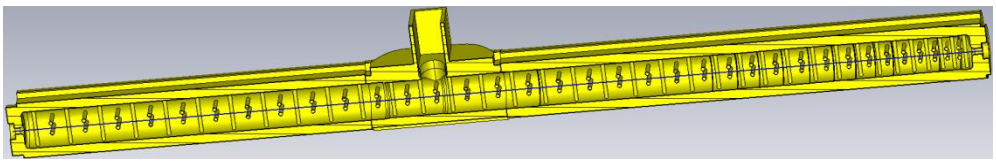

Fig.7: Cut-view for RF model of 1 MeV X-band MicroLinac with novel elliptical RF coupler.

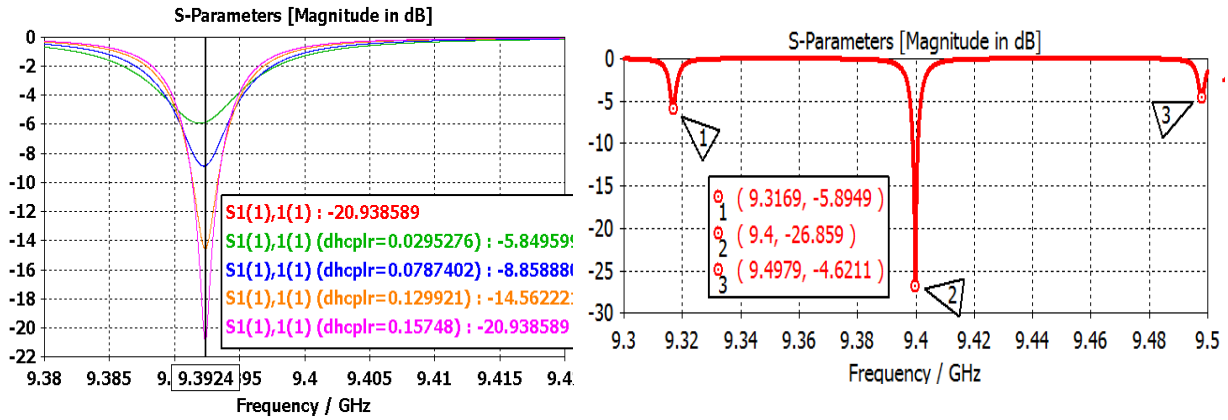

Fig.8: S11 curve simulated for the RF model of Fig.7 for different thicknesses of the coupling wall (left) and the same plotted in wider frequency range (right) for one of the design variants.

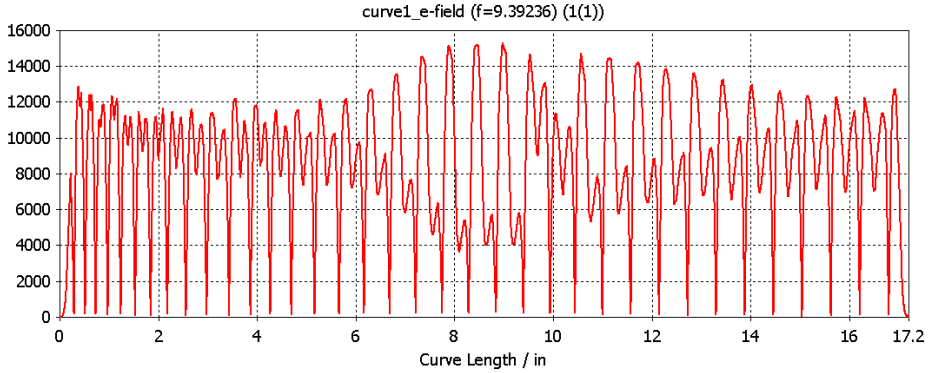

Fig.9: Absolute value of the longitudinal electric field profile plotted along the RF model of Fig.7 for operating mode.

The ~50 MHz frequency separation seen in Fig. 8 is about twice lower than the bandwidth (for phase velocity 0.94) divided by number of cells. This difference is caused by strong tapering of phase velocity on a substantial part of the section, interferences, and presence of RF coupler.

3.1.1. Vacuum simulations

The structure of Fig.7suggests significant vacuum conductivity exceeding most of RF structures at comparable shunt impedance. It may use one or more vacuum ports. We have simulated vacuum performance of the structure with just one vacuum port as shown in Fig.10. For vacuum simulations we applied thermal model using the same approach applied earlier [15,20]. The model parameters of temperature, heat, heat conductance, and heat density on the boundaries correspond to pressure, gas flow rate, vacuum conductance, pumping speed, and outgassing rate respectively. Important to note that this approach can be applied only if mean free path for molecules is much smaller than the internal diameter of the vacuum tube.

The results for the pressure distribution are presented inFig.10. The simulations are performed for 35 l/s pumping speed and $6 \cdot 10^{-8}$Torr·cm^2·l/s outgassing rate for all surfaces (worst case scenario). One can see the maximum pressure simulated is $3.8 \cdot 10^{-7}$Torr.

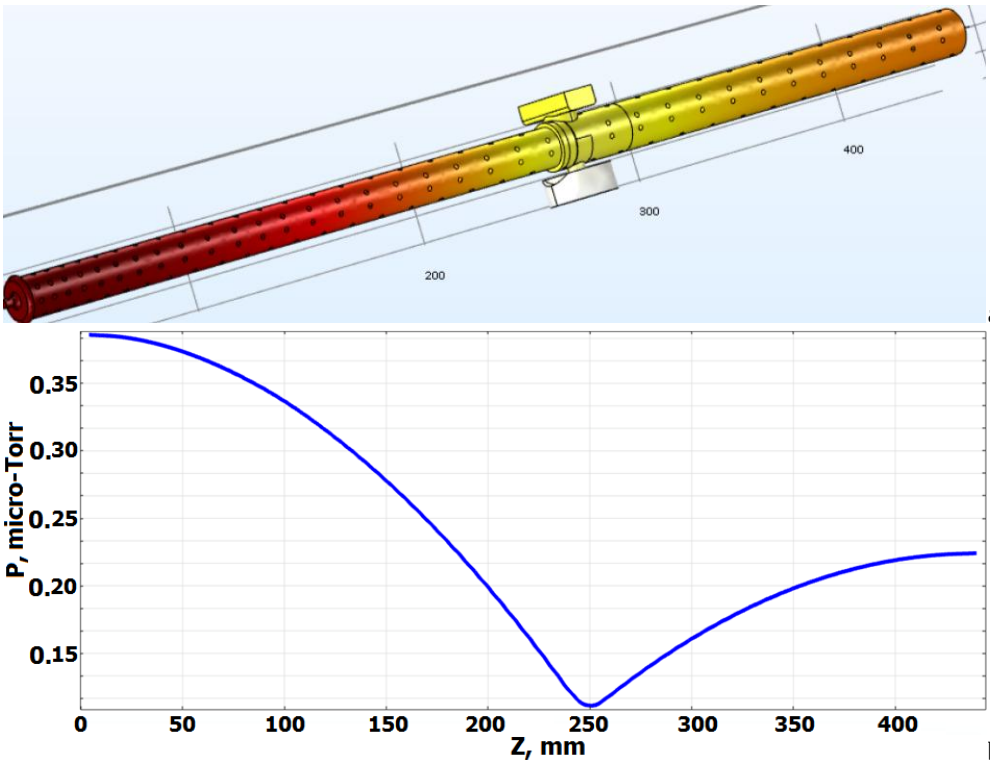

Fig.10: "Negative" volume model (a) for vacuum simulations of the cross-rod MicroLinac section of Fig.7 having just one port for pumping. Pressure distribution simulated along the section (b).

3.2. A 100-cellsingle sectionlinac

Extraordinary wide (>40 MHz) frequency separation between the adjacent modes seen in Fig.8 suggests a much longer SW section to attain energy of several MeVsusing still very limited RF power. Such a ~100-cell long (~1.3m for 9.4 GHz) variant designed for Cs137 replacement is shown in Fig.11. The S11 curves and field profile along the long section are shown in Fig.12a,b and Fig.12c respectively. One can see that the frequency separation between the operating adjacent modes is still substantial (~32 MHz) for such a long section. This value is closer to the rough estimate ~37 MHz obtained for constant geometry (at phase velocity 0.94 without coupler) due to relatively shorter fraction of strong tapering vs, the 37 cell structure above. The modal spectrum seen in Fig. 12b is not uniform because of presence of structure tapering and coupler.

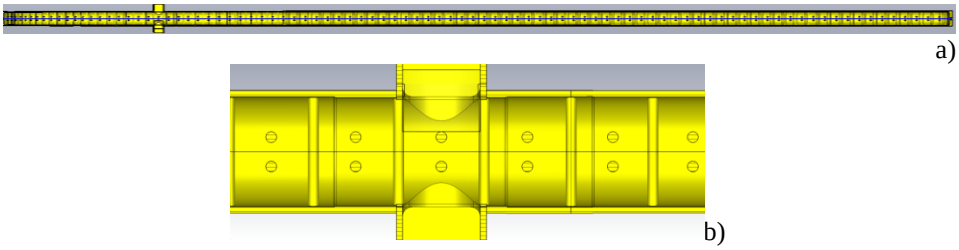

Fig.11: Cut-view of the RF design of a 1.3 m long, cross-rod X-band linac section (a) with two-way coupler(b).

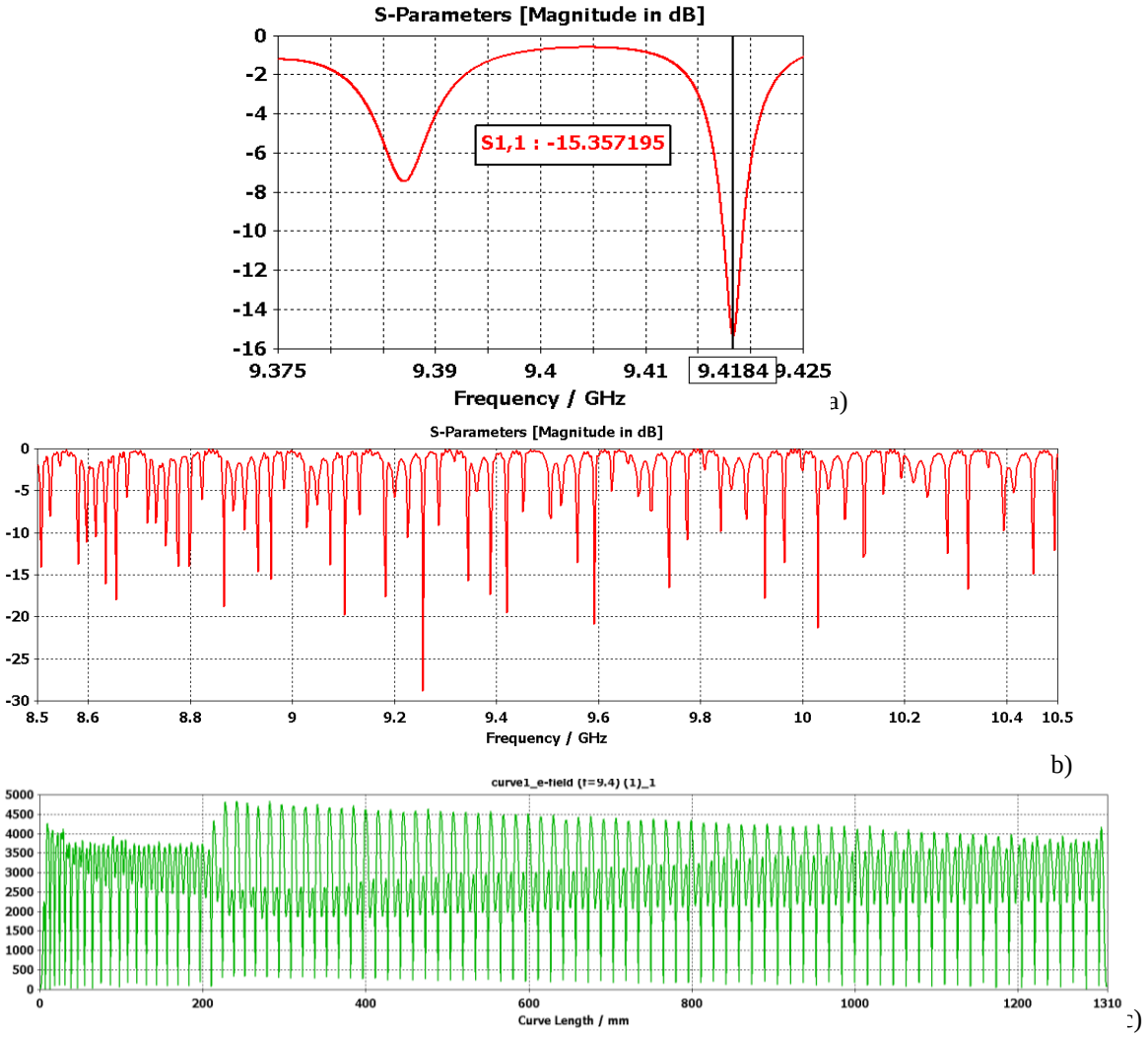

Fig.12:S11-curvessimulated in frequency and time domains respectively (a,b) and longitudinal electric field magnitude (c) plotted along the linac section of Fig.11**.**

Note, unlike DaR structures [14,15] having also substantial bandwidth, the coupler position in the cross-rod section does not affect significantly the field profile as well as beam dynamics considered below. Stable and relatively uniform field distributions occur for different design variants with tree ports, two ports, and single port located in different positions (including the very first cells with lowest β_{ph}).

IV. Beam Dynamics And Focusing Means

Beam dynamics results below are obtained for DC thermionic injection at 14 kV voltage and ~∅3 mm beam waist diameter at the entrance into the structure. Transverse beam emittance is ~1.5 mm·mrad determined by ~(1800-2000)°C dispenser cathode temperature and ~∅6 mm cathode diameter.

The structures under scope do not provide sufficient RF focusing. Basefocusing variant utilizes the same solenoidal type of focusing implemented with permanent magnet blocks in prior MicroLinac designs [6,15]).

4.1. Beam dynamics in the 37-cellsingle sectionlinac

Beam dynamicsresults simulated with ASTRA code [12] for the design of Fig.7are shown in Fig.13 and Fig.14using the field profile of Fig.9 for magnetic field on-axis magnitude 0.15 T.

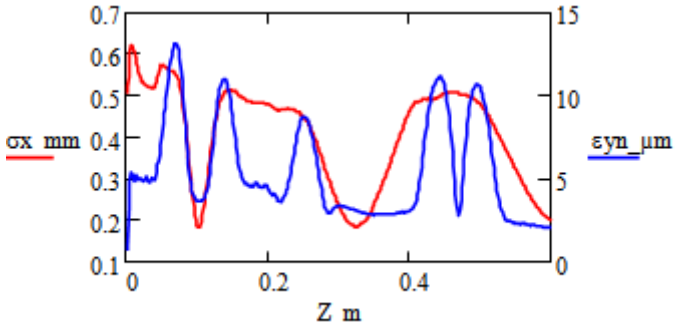

Fig.13: RMS Emittance (blue, right ordinate) and beam rms dimensions (red, left ordinate) simulated with ASTRA code for the field profile of Fig.9. Ez field magnitude is ~7 MV/m.

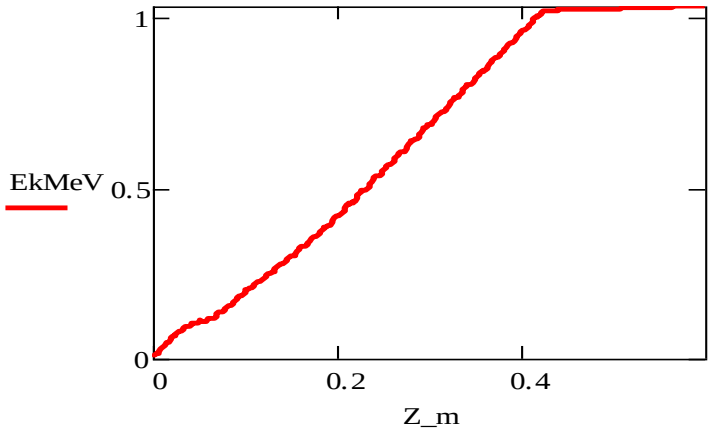

Fig.14: Beam energy gain [MeV] along the structure simulated with ASTRA code for the field profile of Fig.9. Ez field magnitude is ~4.5 MV/m, RF power 100 kW, capture ~15%.

Note ASTRA code has been employed in 2D configuration, whereas the RF structure is not axially symmetric. Therefore we have undertaken 3D PIC simulation of the beam dynamics using corresponding CST Suite solver. The ASTRA 2D results above have been confirmed (see Fig.15).

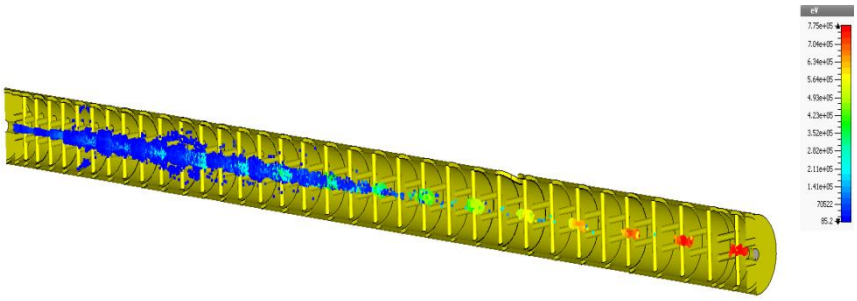

Fig.15: 3D PIC beam dynamics simulated for design of Fig.7with Particle Studio solver of the CST Suite.Maximum on-axis longitudinal electric field is 5 MV/m,RF power is ~70 kW.

4.1.1. Beam dynamics with mild steel pins

An interesting opportunityisrelated to the pins if being made from a copper-plated mild steel. The pins have been included into the full magnetic model (using the same PM-based solenoid). The resulting longitudinal component of the magnetic field along the section is plotted Fig.16. Presence of such an "iron jungle"has led tothe following effects: a) magnetic field magnitude increase by ~16%; and b) local enhancement of transverse fields related to strong derivatives of the local fields.

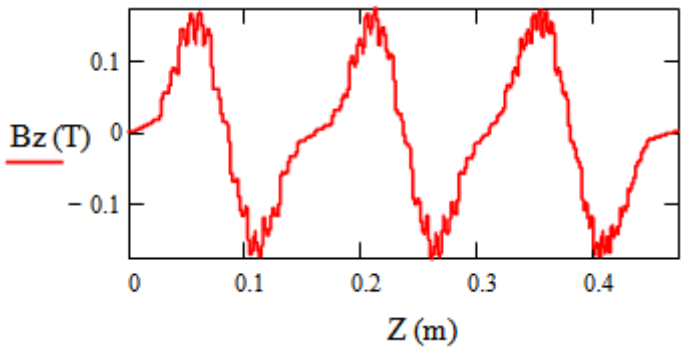

Fig.16:Magnetic field profile along the axis perturbed by the pins made from mild steel and inserted into external focusing field**.**

Beam dynamics simulations results for that case are given in Fig.17. The ASTRA results indicate significant increase beam capture by 32% (at a somewhat lower energy 0.8 MeV).

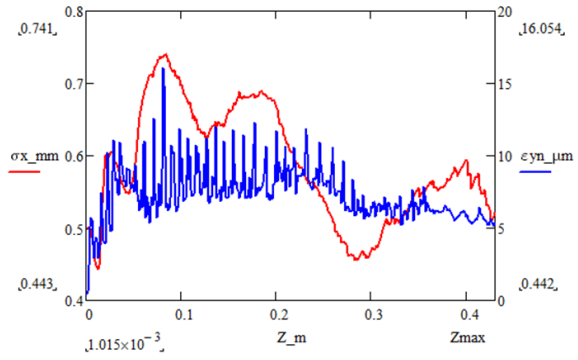

a)

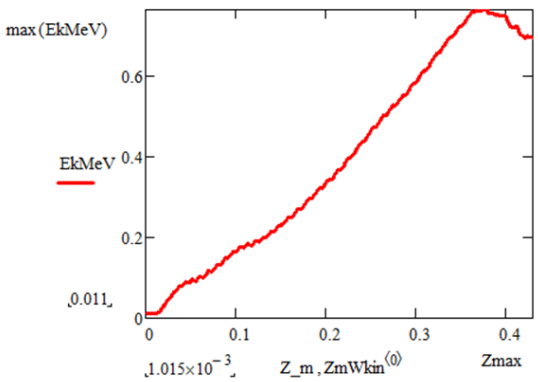

b)

Fig.17:RMS Emittance (blue, right ordinate) and beam rms dimensions (red, left ordinate) simulated with ASTRA code (a). Energy gain along the section of Fig.7with focusing field profile given in Fig.16 and field magnitude ~0.15 T.

4.1.2. Beam dynamics with magnetized pins without external magnet

The results above with pins suggest "zero-weight" focusing using pre-magnetized pins only (i.e. without any external focusing). For example, the pins can be magnetized externally by 7 groups as shown

inFig.18. In Fig.19 we simulated capture coefficient for linac focusing provided by magnetized pins of Fig.18 vs. the on-axis field magnitude.

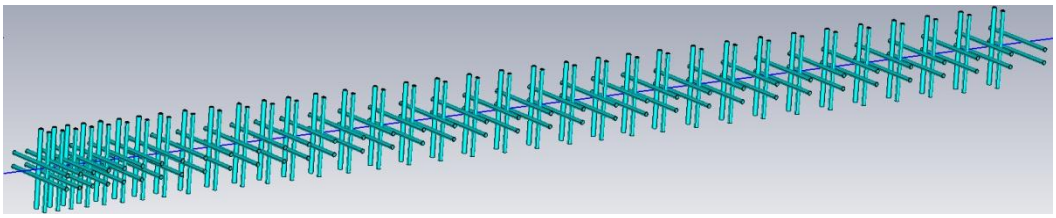

a)

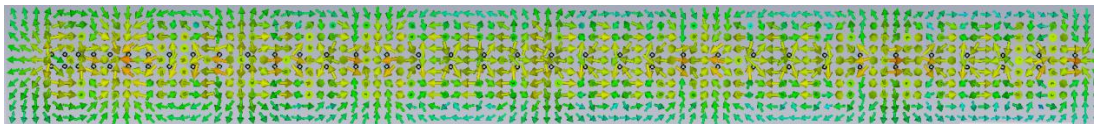

b)

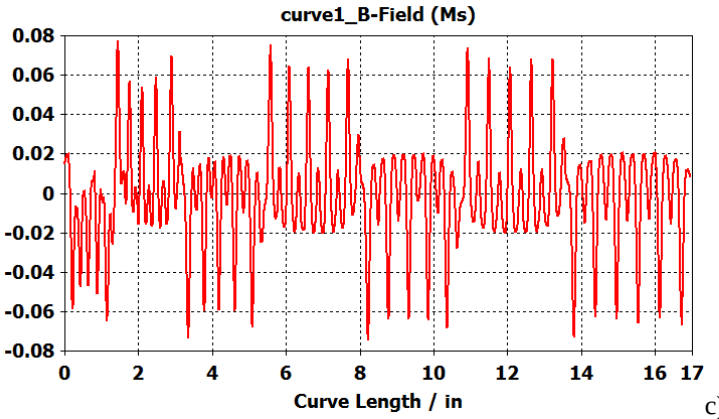

c)

Fig.18: Focusing system provided by magnetized pins made from mild steel (a), the cut-view of the field map (b), and example of the magnetic field profile along the system of alternatively magnetized groups of pins (c).

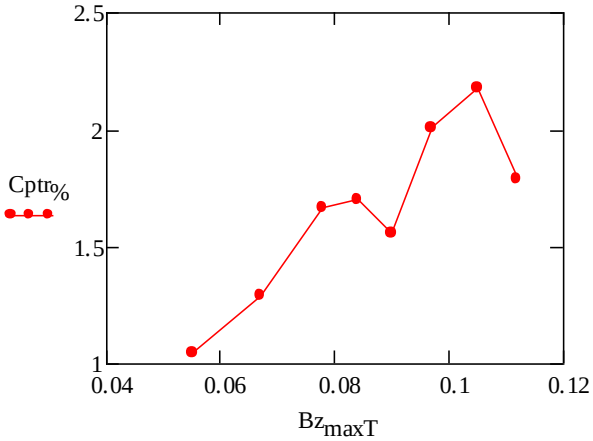

Fig.19: Capture coefficient [%] for linac focusing provided by magnetized pins only using the 17" long setup of Fig. 18 vs. the on-axis field magnitude [T].

Though the capture coefficient calculated in Fig.19 is an order lower than that with external magnet, such a focusing can still be employed in low current applications.Among such applications are X-ray sources with low dose rates, e.g., well logging and non-destructive testing). Besides,capture coefficient can be improved, as the focusing profile of Fig.18c is not optimized.

4.2. Beam dynamics in the 100-cellsingle sectionlinac

For the long linac we apply an alternating solenoid focusing system shown in Fig.20a. The simulated magnetic field is plotted in Fig.20b.

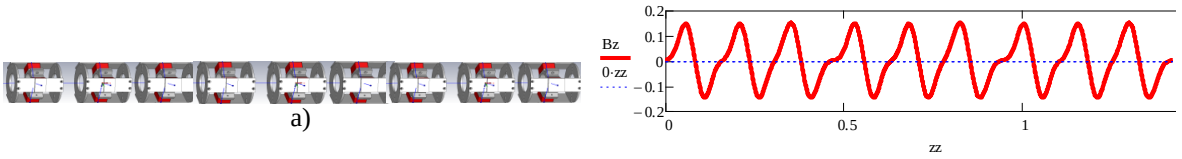

a) b)

Fig.20. PM-based alternating solenoid focusing system (a) and plot of longitudinal magnetic field along the linac (b).

To simulate and analyse beam dynamics we applied the RF fields of Fig.12b along with the magnetic fields of Fig.20b. As it can be seen from

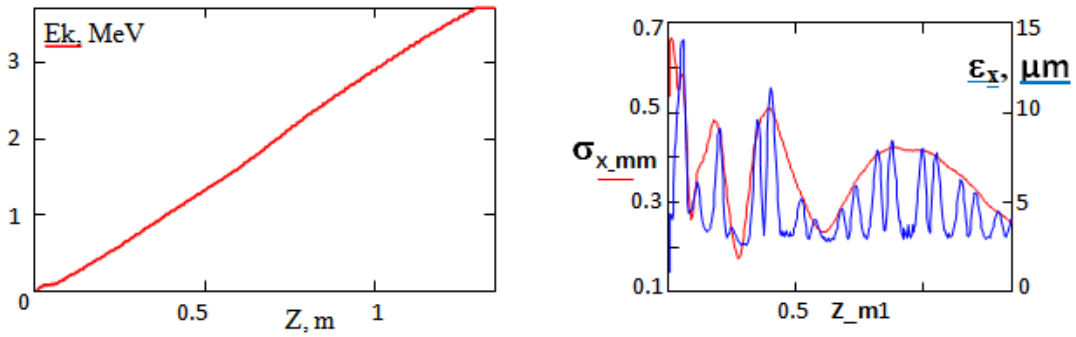

a) b)

Fig.**21**a,b the ASTRA simulations resulted in 3.72 MeV output energy and 15% capture coefficient.

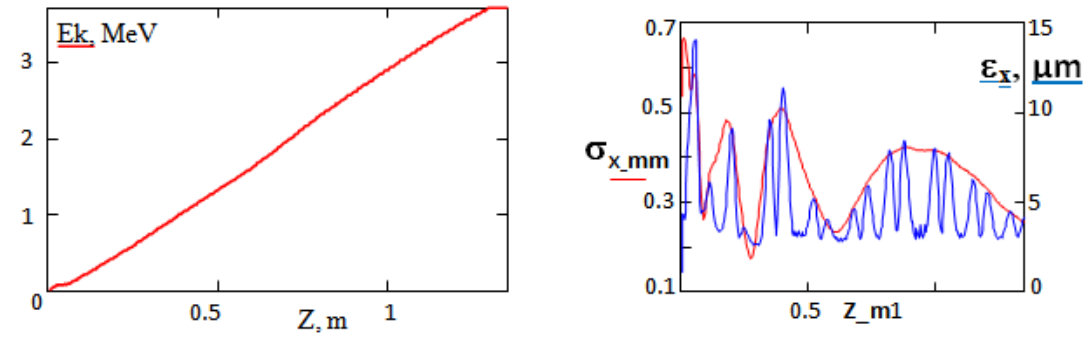

a) b)

Fig.21. Kinetic energy [MeV] (a), beam rms size and transverse emittances (b) plotted along the linac section [m]. PIC simulations of the beam dynamics with CST Suite (c).The pulsed microwave power is 575 kW, at the self-adjusted frequency (~9.4 GHz). Magnetic field is given in Fig.20b.

The results given in

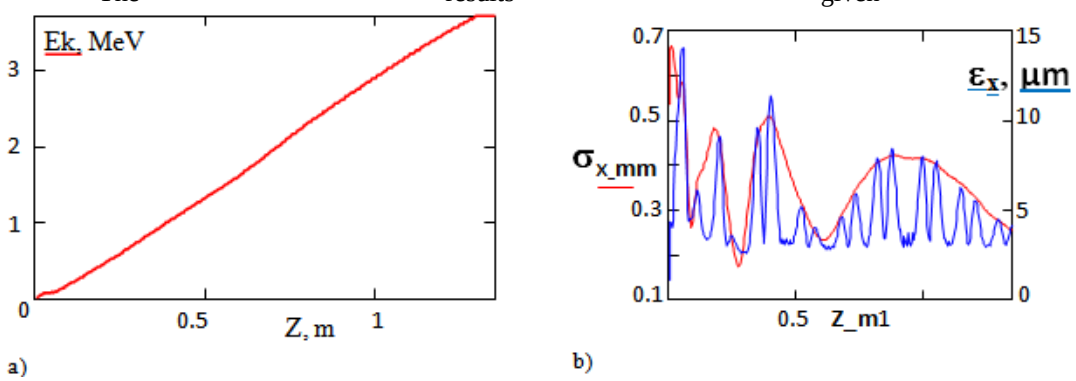

a) b)

Fig.**21**b indicate that design of the focusing system can be optimized further or simply shortened to reduce weight and cost of the system (using, e.g., pins made from mild steel as discussed in Sections 4.1.1 and 4.1.2.).

Preliminary estimations for beam break-up (BBU) we made using the analytical BBU model [21] indicate that the BBU threshold current significantly exceed the currents we consider here for MicroLinac applications (typically limited by ~20 mA during macropulse).

V. Discussion

The multi-cell SW cross-bar and cross-rod structures considered here demonstrate a strong potential for small linacs with beam energies well above 1 MeV at limited power of RF source by simple increasing number of compensated cells due to extraordinary wide bandwidth. A particular feature of the structure enabling these capabilities is a very high group velocity exceeding well 0.2catcorrespondingly high coupling coefficient (up to 0.4) between structure cells. The strongcoupling between cells provides large separation between adjacent modes, field flatness, and field profile robustness with respect to manufacturing inaccuracies. For standing wave (SW) linacs that capability may allow to avoid tuning of structure cells as well as simplify design and ruggedize operation the automatic frequency control (AFC) system. The wide bandwidth makes the structure a viable candidate for harsh environment applications with elevated temperatures and vibrations. Among such applications is well logging using MicroLinac as a replacement of Cs137 logging tools.

A high vacuum conductivity of the structure suggests effective usage of non-evaporable getter pumps (NEGs): low pumping speed required can make such a system very compact (from one to three discrete ports can be used). The jungle-gym multi-cell structure can be more attractive than on-axis coupled (e.g., circular disk loaded) structures in terms of compactness as well asperformance to cost ratio for decimeter through centimetre wavelengths.The structures considered here allow elimination of tuning of individual cells. The bars and rods can use inexpensive pins and profiles available commercially. Shunt impedance of a typical circular disk loaded structure for a MicroLinac [5,6] is a somewhat between cross-rod structure and cross-bar structure. However, too dense modal spectrum and difficulty to tune field profile in a conventional narrow-band structure make it problematic for application in long multi-cell designs.

The maximum internal diameter of the cross-bar (or cross-rod) structures is typically ~0.5-0.6 wavelength (dependently on particular geometry and phase velocity).Such compactness is similar to spoke cavities as well as disk-and-ring, disk-and-rod structures. The internal transverse dimension can be compared to $>0.8\lambda$ for conventional disk loaded structure, which also requires tuners making the outer diameter even larger. The small transverse dimension is critical for orbit separation in compact racetrack microtrons operating centimetre wavelengths. Devices with velocity bunching (traveling wave tubes, TWTs, and backward wave oscillators, BWOs) can also present a potential area of application. Cross-bar structures offer higher interaction (coupling) impedances than iris loaded structures employed in earlier non-relativistic and later in relativistic tubes [22] (up to about a factor of two dependently on phase velocity) at more than triple wider bandwidth. The compensation in cross-rod structures is similar to that in ring-bar structures [23] enabling even stronger (>0.9) coupling between cells (and hence broader bandwidth). However, ring-bar structures have lower interaction impedance (e.g., <100 Ω vs. >200 Ω at $\beta_{ph}>0.7$) and mechanically are less rigid than the cross-rod/cross-pin structure as require support of the fragile insert suspended in a tubular housing. The stiffness is especially important for harsh environment and mobile applications at short (centimetre) wavelengths when vibrations may occur. The cross-barstructure can also be effectively employed in X-band version of a cascaded BWO-TWT accelerating-generating [24,25] linacfor both BWO and TWT parts (using different spatial harmonics).

Thus the cross-bar and cross-rod structures can be considered as candidates for MicroLinacs capable of replacing of a wide spectrum radioactive sources. The structuresalso offer a certain potential for racetrack microtrons, traveling wave tubes, drivers for mm-sub-mm wave pulsed sources, and RF deflectors employed for phase space manipulation, beam diagnostics, and material spectroscopy with ultrafast electron diffraction.

Acknowledgements

This work was supported by the U.S. Department of Energy (awards No. DE-SC-FOA-0011370 and DE-SC0015721).The authors are especially gratifying to Dr. Ahmed Badruzzaman for his encouraging support of this work potential for well logging in petroleum industry. The authorsare grateful to Dr. Arden Dougan, Dr. Bruce Carlsten, and Dr. Sergey Kurennoyfor theirsupportive interest to that development. The authors appreciate KurbisJunge, Dr. Alex Murokh, Salime Boucher, Dr. Alexander Smirnov and Ronald Agustsson for discussions related to performance, packaging, fabrication, engineering, and testing of a MicroLinac system. The authors are thankful to Prof. V.V. Paramonov on the fundamental correction made regarding vacuum simulations.

References

[1]. A. V. Smirnov.In*Proceedings of North-American Particle Accelerator Conference (NA-PAC'13),* Pasadena, CA USA (2013) 1421.

[2]. "Radiation Source Use and Replacement: Abbreviated Version," Sciences Committee on Radiation Source Use and Replacement, National Research Council (2008).

[3]. N. Ackerman et al., "MicroLinac – A Portable Accelerator for Radiography", *The 12th Advanced Accelerator Concepts Workshop*, 2006.

[4]. T. Yamamoto, T. Natsui, F. Sakamoto, M. Uesaka, N. Nakamura and E. Tanabe, "Development of portable X-band linac X-ray source for non-destructive testing", *Proceedings of the Joint International Workshop: Nuclear Technology and Society–Needs for Next Generation*, Berkeley, California, 2008.

[5]. S. Boucher, X. Ding, A. Murokh, In *Proceedings of Intern.Particle Accelerator Conf. (IPAC'10)* Kyoto, Japan (2010) 178.

[6]. S. Boucher, R. Agustsson, L. Faillace, J. Hartzell, A. Murokh, A. Smirnov, S. Storms, K. Woods. *Proceedings of Intern.Particle Accelerator Conf. (IPAC2013)* Shanghai, China (2013) 3746.

[7]. R.P. Borghi, A.L. Eldredge, G.A. Loew and R.B. Neal.Design and Fabrication of the Accelerating Structure for the Stanford Two-Mile Accelerator.*SLAC-PUB-71*, 1963.

[8]. M. Tigner, Bar Loaded Waveguide for Accelerator Service, *IEEE Trans. Nucl.Sci., NS-18 No.3* (1971).

[9]. J. Loo, M. J. Browman, K. C. D. Chan, and R. K. Cooper. *Particle Accelerators, 1988, Vol. 23*, pp. 279-287.

[10]. A. V. Smirnov.*Nuclear Instruments and Methods in Physics Research A 572* (2007) 561–567.

[11]. https://www.cst.com/2015

[12]. *Astra - A space charge tracking algorithm*. User's manual. Version 3.0, DESY, Hamburg, 2011.

[13]. V. G. Andreev et al., *Proc. Intern. Conf. on High Energy Accelerator, (Frascati, Italy, 1965); Soviet Physics - Technical Physics 1*3 (1969) 1070.

[14]. A. V. Smirnov and E. Savin, *Nuclear Inst. and Meth.NIM A, vol. 820, N1* (2016) 48-53.

[15]. A.V. Smirnov, S. Boucher, S. Kutsaev, J. Hartzell, E. Savin.*Nuclear Inst. and Meth.NIM A, V 830, 11*, 2016, 294–302.

[16]. J. R. Delayen, *Proc. of Linear Accelerator Conf. (LINAC'88)* Newport News, Virginia, US (1988) 199.

[17]. http://epaper.kek.jp/LINAC2010/talks/tu302_talk.pdf

[18]. D. Gorelov et al., *Proceedings of IPAC2012*, New Orleans, Louisiana, USA (2012) 2408.

[19]. http://accelconf.web.cern.ch/accelconf/srf2015/talks/wea2a01_talk.pdf

[20]. H.J. Lee, C. H. Yi, S. H. Kim, M. H. Cho, W. Namkun, C. D. Park, in *Proceedings of IPAC 2011*, San Sebastian, Spain (2011) 1548.

[21]. A. V. Smirnov.*Nuclear Inst. and Meth.NIM A, vol. 589* (2008) pp. 13-19.

[22]. T. Kimura, S. Alberti: B.G. Danly, and R.J. Temkin.In*Proc. of Part. Acc. Conf. PAC'93* (1993) 2690-2692.

[23]. M. Zuboraj.*Coupled Transmission Line Based Slow Wave Structures for Traveling Wave Tubes Applications*. Ph. D. Dissertation, Ohio State University, USA, 2016.

[24]. A.V. Smirnov, V.N. Smirnov.*Nucl.Instrum.and Meth. NIMA349*(1994) 614-617.

[25]. A.V. Smirnov, V.N. Smirnov.*Rev. Sci. Instr., RSI 66, N3 (1995)* 2552-2561.